Letter

Engineered Diffraction Gratings for Acoustic Cloaking

Yabin Jin,[1,‡] Xinsheng Fang,[2,3,‡] Yong Li,[2,3,*] and Daniel Torrent[4,†]

[1] *School of Aerospace Engineering and Applied Mechanics, Tongji University, 200092 Shanghai, People's Republic of China*

[2] *Institute of Acoustics, School of Physics Science and Engineering, Tongji University, 200092 Shanghai, People's Republic of China*

[3] *Shanghai Key Laboratory of Special Artificial Microstructure Materials and Technology, School of Physics Science and Engineering, Tongji University, 200092 Shanghai, People's Republic of China*

[4] *GROC, Institut de Noves Tecnologies de la Imatge, Universitat Jaume I, 12071 Castelló, Spain*

(Received 3 September 2018; revised manuscript received 29 October 2018; published 25 January 2019)

We show that engineered diffraction gratings can considerably simplify the design of acoustic ground cloaking devices. Acoustic reflecting gratings are designed in such a way that all the incident energy is channeled toward the diffracted mode traveling in the direction opposite the direction of the incident field (retroreflection effect), and this effect is used to cloak an object placed over an acoustically rigid surface. Axisymmetric gratings consisting of rigid surfaces with just one groove per unit cell are used to design thin acoustic carpet cloaks. Finally, full-wave numerical simulations are performed and a conical carpet cloak is experimentally tested, showing an excellent scattering-cancellation effect.

DOI: 10.1103/PhysRevApplied.11.011004

Acoustic cloaking [1] is one of the most-challenging problems related to classical wave control. It is directly related to the original idea of electromagnetic cloaking [2], and a huge amount of research has been devoted to theoretically and experimentally solving this problem, the requirement of single parameters being one of the major milestones to achieve the realization of these devices. The so-called carpet cloak [3], or ground cloak, is a special type of cloaking shell that makes objects positioned on a flat mirror invisible, with the remarkable property of not requiring extreme materials' parameters for its realization. Acoustic carpet cloaks with finite anisotropy and homogeneous materials' parameters can be designed in the framework of acoustic metamaterials. For instance, perforated plastic plates [4,5] and steel-air composites [6] have been proposed to numerically and experimentally study two-dimensional and three-dimensional (3D) carpet cloaks for air-borne acoustic wave propagation. In underwater acoustics, layered mercury inclusions [7] or brass plates [8] were considered to theoretically design carpet cloaks, which have recently been experimentally demonstrated by design of a steel-stripe-composited pyramid [9]. Finally, carpet cloaks have also been explored for other types of mechanical waves, such as water [10] or elastic [11] waves. However, the size of the carpet-cloak shell compared with that of the cloaked region is still large, which limits the potential applications of these devices.

With the advent of metasurfaces [12–14], which are artificially structured thin surfaces capable of modulating the reflected wavefronts, a new type of carpet cloak was envisaged. Thin carpet cloaks based on Helmholtz resonators [15–17], membranes [18,19], and spiral cavities [20] were designed in this framework. However, the main constraint of these structures is that metasurfaces are complex periodically structured surfaces in which the complexity of the unit cell strongly hinders their effectivity, since only very small cloaks with a small number of periods are feasible from the practical point of view. Additionally, the need for a large number of resonators forces the devices to work at very low frequencies and dissipation is a major drawback in their functionality.

In this work an engineered grating [21–23] is applied to the simplified design of acoustic carpet cloaks, and it is shown that these can be built with gratings having only one cavity per unit cell, which is much simpler than the approaches based on metasurfaces, which require a large number of resonators per unit cell. Experiments are performed to illustrate the functionality of these devices, showing that this simplified approach may open new lines in the design of more-advanced devices for the control of acoustic and other waves.

Figure 1 shows a schematic representation of the idea developed in this work. The upper panel shows a diffraction grating operating at a wavelength such that, for a

*yongli@tongji.edu.cn
†dtorrent@uji.es
‡Y.J. and X.F. contributed equally to this work.

specific incident angle θ_0, we have only two reflected modes: the fundamental one is specularly reflected and has amplitude B_0; and the $n=-1$ mode, which has amplitude B_{-1}, is "retroreflected" [22,24]. This condition can be achieved according to the diffraction condition

$$\sin\theta_n = \sin\theta_0 \pm \frac{2n\pi}{ka}, \tag{1}$$

where k is the wavenumber of the incident plane wave and a is the lattice constant of the grating. The angle θ_n is the angle of the diffracted wave. For a propagating wave we require that $|\sin\theta_n| \leq 1$, which for a given k happens only for a finite number of modes ($n = N_P$). The grating shown in Fig. 1 is designed in a way that only the $n = 0, -1$ modes are propagative, with the additional condition that $\sin\theta_n = -\sin\theta_0$, which defines the operating ka value as

$$ka = \frac{\pi}{\sin\theta_0}. \tag{2}$$

The grating consists of periodically drilled cavities of length L_0 and width d_0 in an acoustically rigid surface. It can be shown that with only one cavity per unit cell it is possible to engineer the grating in such a way that the amplitude of the specular reflection $B_0 = 0$; therefore, all the reflected energy goes to the diffracted mode $n = -1$ and the grating acts as a perfect retroreflector. The equation that has to be satisfied for the design of such a grating was shown in Ref. [22] to be

$$\cot kL_0 = \frac{d_0}{a}\sum_{n\neq 0,-1}\frac{k}{|q_n|}\mathrm{sinc}^2\left(\frac{|\mathbf{k}a + 2\pi n\mathbf{x}|d_0}{2a}\right) \tag{3}$$

where $\mathbf{k} = k(\cos\theta_0\mathbf{x} + \sin\theta_0\mathbf{z})$ is the incident wavenumber and $q_n = \sqrt{k^2 - |\mathbf{k} + 2\pi n/a\mathbf{x}|^2}$.

We can now give the shape of the grating illustrated in the lower panel in Fig. 1, which is a conical surface whose angle is identical to satisfy the retroreflection condition, so that any wave arriving from the top with a wavevector parallel to the axis of the cone will be retroreflected in the vertical direction, canceling the scattering toward the x-y plane. Consequently, it cloaks the conical object, since the scattering direction will be the same as it would be if the conical object were not there.

Figure 2 shows the length of the groove L_0 relative to the operating wavelength λ that we need to satisfy the retroreflection condition as a function of the angle of incidence θ_0. The minimum incident angle that allows this condition to be satisfied is given when the $n = 1$ mode begins to be propagative, which corresponds to $\sin\theta_0 = 1/3$, or $\theta_0 \approx 20^\circ$. Results are shown for different groove widths d_0, and the dotted yellow line corresponds to $d_0/\lambda = 0.3$, which is the thickness we use in our work. It is clear that the trends of the length L_0 are very similar and the variations are quite smooth, which is interesting from the experimental point of view as well, since it shows that deviations due to fabrication errors will not affect excessively the retroreflection effect.

Figure 3 shows full-wave simulations performed with COMSOL MULTIPHYSICS of different cloaks designed with this approach, assuming an axisymmetric geometry. A

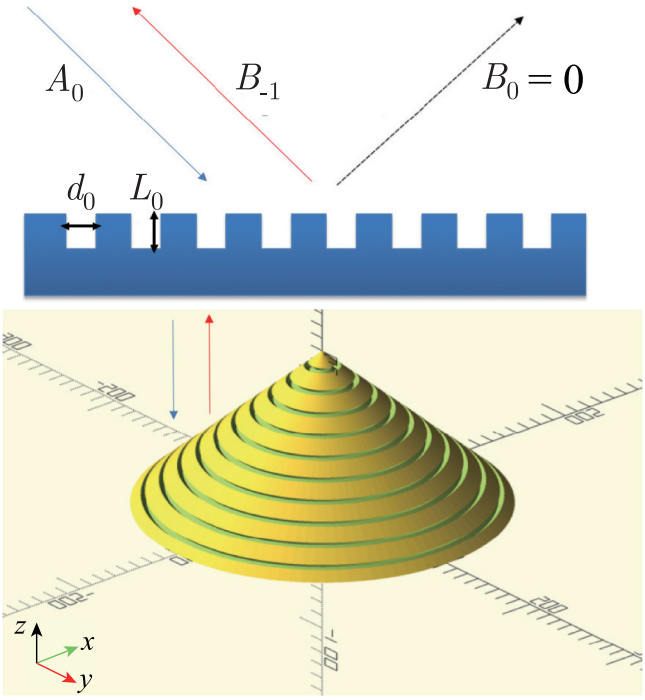

FIG. 1. The structure considered in this work. An acoustic grating (upper panel) is designed in such a way that only the $n = -1$ mode is excited, the specularly reflected mode being canceled. If we give this grating a conical shape (lower panel), we can use it as a carpet cloak.

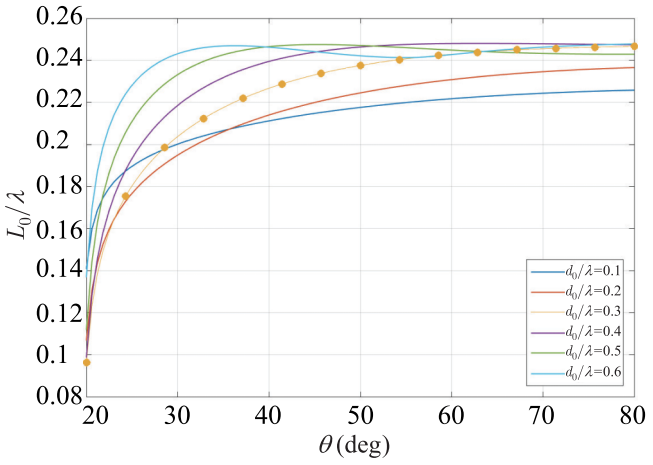

FIG. 2. Required cavity length L_0 as a function of the angle of incidence to cancel the specular reflection of the grating for different values of the cavity width d_0.

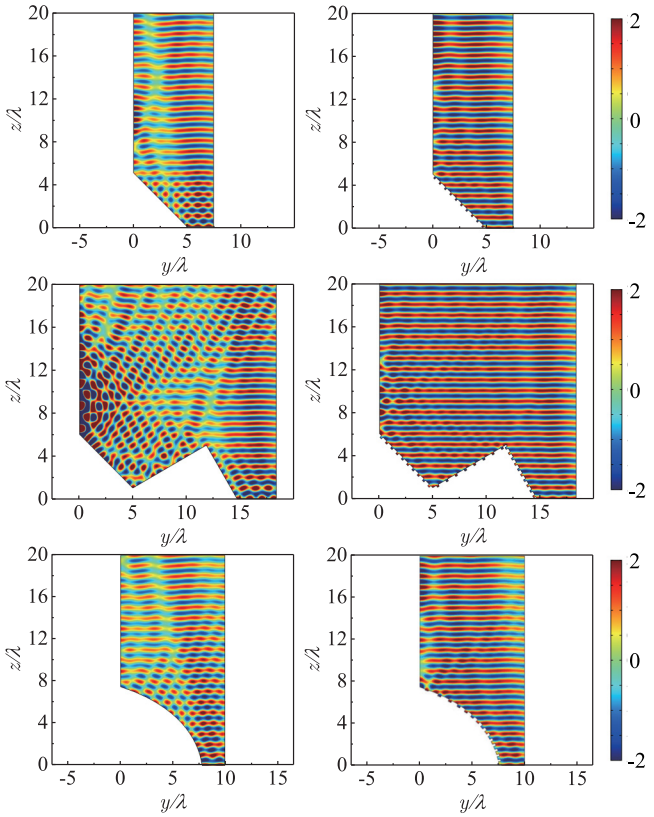

FIG. 3. Different carpet cloaks based on an engineered diffraction grating. The left plots show the scattering due to the flat object and the right plots show the scattering from the same surface with a drilled grating. We can see perfect performance of the cloak for a single-angle grating (top panel), a three-angle grating (middle panel), and a multiangle grating (bottom panel).

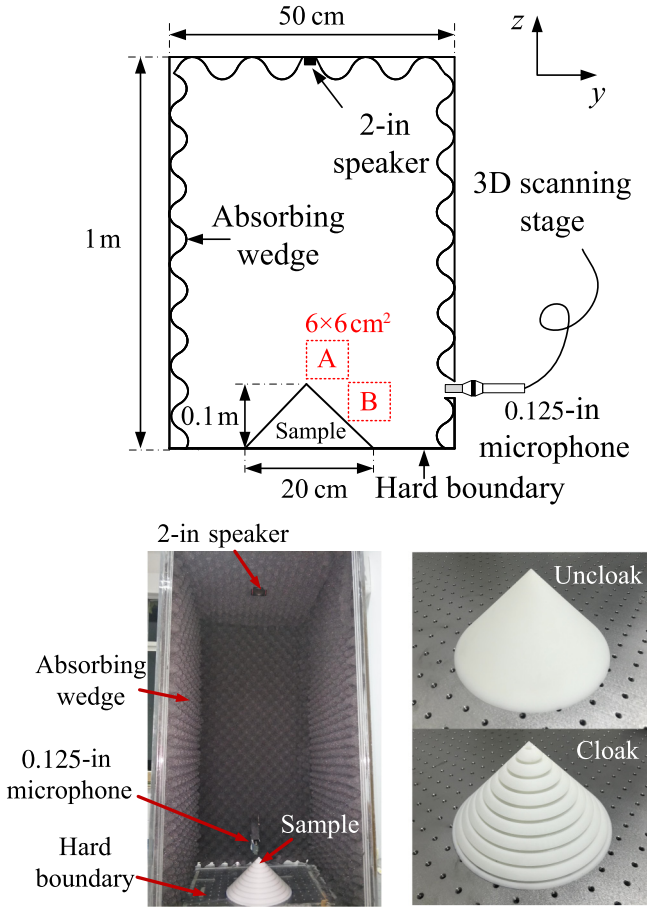

FIG. 4. The experimental setup (upper panel) and pictures of the samples and the chamber (lower panel). 3D, three-dimensional.

plane wave parallel to the vertical axis (the z axis) arrives from the top of the figure and is scattered by the objects placed over an acoustically rigid base. The top panel shows the same conical structure discussed before, with the conical surface making an angle $\theta_0 = \pi/4$ with the vertical axis and the propagation direction of the incident field. The left plot shows the scattering of this object with a rigid surface and the right plot shows the cloak effect due to the efficient grating design. Clearly the scattering toward the horizontal direction, which corresponds to the specular reflection, has been completely canceled, and only the retroreflection is observed, with an obvious cloaking effect. The middle panel shows that the grating does not need to be uniform to perform the cloaking effect properly, and in this case there are three different angles of the surface that correspond to three different angles of incidence ($\theta_0 = \pi/4, \pi/6$, and $\pi/3$); therefore, each surface will have a different length L_0 of the grooves. As before, the scattering due to the flat surface (left plot) is completely canceled by the grating (right plot). Finally, the bottom panel shows a nearly curved surface in which each angle contains a unit cell, so each of these surfaces has a different groove length. The retroreflection effect is clear here as well, as can be seen due to the cancellation of the scattering by the cloak. It is interesting that, although the design is based on diffraction gratings, which are periodically structured surfaces, the effect still remains even when we use only one unit cell, where we change locally not only the angle of the surface but also the period of the cell, which illustrates the possibilities of this approach to cloak both large-area surfaces and small local defects.

Although these cloaking devices are designed for normal incidence and for a specific frequency, small deviations from both the angle of incidence and the operating frequency will cause only small deviations from the perfect operation. This is because the dependence of the amplitude of the specular reflection around its cancellation condition as a function of both the incident angle and the frequency is smooth, as can be seen in Ref. [22], so deviation from the "perfect" operation will also be smooth.

The cloaking effect is tested experimentally by means of the first example in Fig. 3. We fabricate samples by use 3D-printing technology, via laser-sintering stereolithography

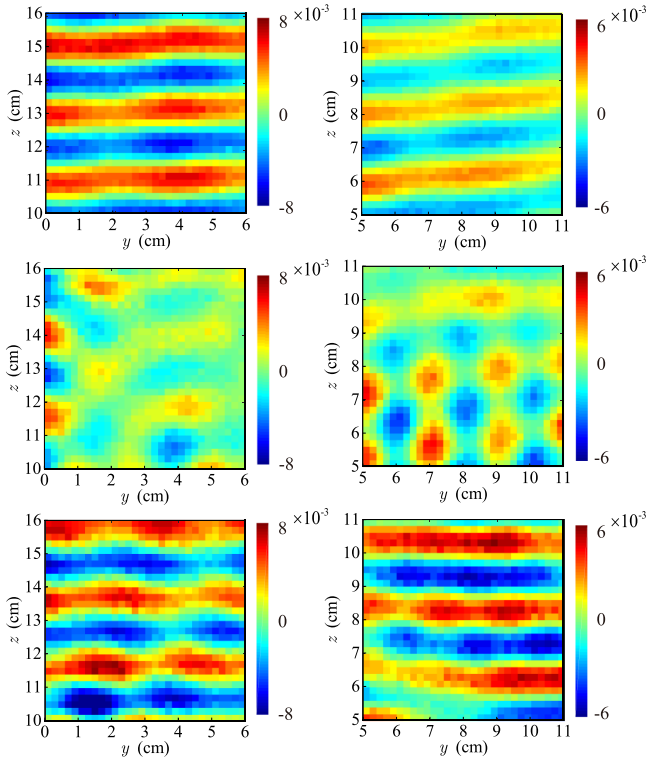

FIG. 5. Experimental measurements of the real part of the acoustic field in region A (left) and region B (right) shown in Fig. 4. We can see how a plane wave is excited and measured without an object (top panel). This wave is scattered when we place the flat conical surface shown in Fig. 4 (middle panel), and when the conical surface is structured by the grating, the scattered field almost disappears (bottom panel).

and with photosensitive resin, where the manufacturing precision is 0.1 mm. The thickness of the sample is 8.6 mm, including the hard boundary. The ratio between the thickness and the wavelength (the frequency is 17 kHz in the experiment) is about 0.426. The wave-field mapping measurements are performed in a man-made anechoic room ($0.5 \times 0.5 \times 1$ m^3) with absorbing wedges (thickness 5 cm) installed on the walls. A continuous sound wave with a center frequency of 17 and 6.4-kHz span is emitted from a 2-in. loudspeaker located on the top of the anechoic room. A 0.125-in. Brüel & Kjær microphone (model 2670) is connected to a three-dimensional moving stage to record the pressure fields. The measured signal from the microphone and the source signal are connected to the Brüel & Kjær LAN-XI data-acquisition hardware (model 3160-A-042) to obtain the amplitude and phase of the mapping pressure fields. To reveal the invisibility effect of the acoustic cloak, we measure two rectangular regions (A and B, as shown in Fig. 4) on the top and on the right of samples, respectively. The measured regions (6×6 cm^2) are meshed into 900 squares with a spacing of 2 mm.

Figure 5 shows the experimentally measured wave forms for scanning region A (left) and scanning region B (right). When there is no sample in the chamber (top panel), a nearly plane wave propagates in free space. Once we place the uncloaked object (middle panel), this free field is strongly scattered, and a clear interference pattern can be seen, especially in region B. When the uncloaked object is replaced by the cloak, we see how the free field is nearly recovered (bottom panel), canceling the scattered field toward the undesired direction. The simplicity of this device in comparison with other devices with similar functionalities is remarkable, which allows us to build a relatively large sample with strong scattering cross section, as can be seen from both the simulations and the experimental measurements shown in Figs. 3 and 5.

In summary, we demonstrate that engineered diffraction gratings can be used to efficiently design carpet cloaks, with the remarkable property of being simpler structures than those presented so far in the literature. It is shown that the grating properties remains even when the geometry of the grating is modified, for example, giving it a conical shape or changing locally the period of the grating, which allows us to design three-dimensional axisymmetric cloaks with different shapes. The conical cloak is experimentally tested and excellent functionality is observed. The results obtained in this work can be easily exported not only to other mechanical waves but also in the electromagnetic domain, where cloaks and similar devices based on complex metasurfaces are currently being investigated.

ACKNOWLEDGMENTS

D.T. acknowledges financial support through a "Ramón y Cajal" fellowship under grant number RYC-2016-21188 and by the U.S. Office of Naval Research under Grant No. N00014-17-1-2445. Y.L. acknowledges support from the National Natural Science Foundation of China under Grant No. 11704284 and the Shanghai Pujiang Program under Grant No. 17PJ1409000. Y.L. and Y.J. acknowledge start-up funding from Tongji University.

[1] S. A. Cummer and D. Schurig, One path to acoustic cloaking, New J. Phys. **9**, 45 (2007).
[2] J. B. Pendry, D. Schurig, and D. R. Smith, Controlling electromagnetic fields, Science **312**, 1780 (2006).
[3] J. Li and J. B. Pendry, Hiding under the Carpet: A New Strategy for Cloaking, Phys. Rev. Lett. **101**, 203901 (2008).
[4] B. I. Popa, L. Zigoneanu, and S. A. Cummer, Experimental Acoustic Ground Cloak in Air, Phys. Rev. Lett. **106**, 253901 (2011).
[5] L. Zigoneanu, B. I. Popa, and S. A. Cummer, Three-dimensional broadband omnidirectional acoustic ground cloak, Nat. Mater. **13**, 352 (2014).

[6] X.-L. Zhang, X. Ni, M.-H. Lu, and Y.-F. Chen, A feasible approach to achieve acoustic carpet cloak in air, Phys. Lett. A **376**, 493 (2012).
[7] J. Xiong, T. Chen, X. Wang, and J. Zhu, Design and assessment of an acoustic ground cloak with layered structure, Int. J. Mod. Phys. B **29**, 1550191 (2015).
[8] Y. Bi, H. Jia, W. Lu, P. Ji, and J. Yang, Design and demonstration of an underwater acoustic carpet cloak, Sci. Rep. **7**, 705 (2017).
[9] Y. Bi, H. Jia, Z. Sun, Y. Yang, H. Zhao, and J. Yang, Experimental Demonstration of Three-dimensional Broadband Underwater Acoustic Carpet Cloak, Appl. Phys. Lett. **112**, 223502 (2018).
[10] Z. Wang, C. Li, R. Zatianina, P. Zhang, and Y. Zhang, Carpet cloak for water waves, Phys. Rev. E **96**, 053107 (2017).
[11] P. Zhang and W. J. Parnell, Hyperelastic antiplane ground cloaking, J. Acoust. Soc. Am. **143**, 2878 (2018).
[12] N. Yu, P. Genevet, M. A. Kats, F. Aieta, J. P. Tetienne, F. Capasso, and Z. Gaburro, Light propagation with phase discontinuities: Generalized laws of reflection and refraction, Science **334**, 333 (2011).
[13] Y. Li, B. Liang, Z. M. Gu, X. Y. Zou, and J. C. Cheng, Reflected wavefront manipulation based on ultrathin planar acoustic metasurfaces, Sci. Rep. **3**, 2546 (2013).
[14] Y. Xie, W. Wang, H. Chen, A. Konneker, B. I. Popa, and S. A. Cummer, Wavefront modulation and subwavelength diffractive acoustics with an acoustic metasurface, Nat. Commun. **5**, 5553 (2014).
[15] Y. Yang, H. Wang, F. Yu, Z. Xu, and H. Chen, A metasurface carpet cloak for electromagnetic, acoustic and water waves, Sci. Rep. **6**, 20219 (2016).
[16] C. Faure, O. Richoux, S. Félix, and V. Pagneux, Experiments on Metasurface Carpet Cloaking for Audible Acoustics, Appl. Phys. Lett. **108**, 064103 (2016).
[17] M. Dubois, C. Z. Shi, Y. Wang, and X. Zhang, A Thin and Conformal Metasurface for Illusion Acoustics of Rapidly Changing Profiles, Appl. Phys. Lett. **110**, 151902 (2017).
[18] H. Esfahlani, S. Karkar, H. Lissek, and J. R. Mosig, Acoustic carpet cloak based on an ultrathin metasurface, Phys. Rev. B **94**, 014302 (2016).
[19] S. Zhai, H. Chen, C. Ding, L. Li, F. Shen, C. Luo, and X. Zhao, Ultrathin skin cloaks with metasurfaces for audible sound, J. Phys. D: Appl. Phys. **49**, 225302 (2016).
[20] X. Wang, D. Mao, and Y. Li, Broadband acoustic skin cloak based on spiral metasurfaces, Sci. Rep. **7**, 11604 (2017).
[21] T. J. Cox and P. D'Antonio, Acoustic phase gratings for reduced specular reflection, Appl. Acoust. **60**, 167 (2000).
[22] D. Torrent, Acoustic anomalous reflectors based on diffraction grating engineering, Phys. Rev. B **98**, 060101 (2018).
[23] P. Packo, A. N. Norris, and D. Torrent, Inverse Grating Problem: Efficient Design of Anomalous Flexural Wave Reflectors and Refractors, Phys. Rev. Appl. **11**, 014023 (2019).
[24] G. Y. Song, Q. Cheng, T. J. Cui, and Y. Jing, Acoustic planar surface retroreflector, Phys. Rev. Mater. **2**, 065201 (2018).